Received: November 16, 2023. Revised: February 1, 2024.

International Journal of
Intelligent Engineering & Systems

http://www.inass.org/

The Effect of High-Speed Train Channel on the Performance of DVB-Terrestrial Communication Systems

Anggun Fitrian Isnawati[1]* **Wahyu Pamungkas[1]** **M. Panji Kusuma Praja[1]**

[1]*Institut Teknologi Telkom Purwokerto, Central Java, Indonesia*
*Corresponding author's email: anggun@ittelkom-pwt.ac.id

Abstract: The high mobility associated with high-speed train (HST) results in nonstationary channel conditions that characterized by varying environments leads to challenges like rapid changes in signal strength and quality. As train speeds increase, the Doppler shift occurs and the Peak to Average Power Ratio (PAPR) in the system also increases, which is a common challenge in modulation schemes such as Orthogonal Frequency Division Multiplexing (OFDM). The paper investigates the impact of HST environments on the performance of Digital Video Broadcasting - Terrestrial (DVB-Terrestrial) systems. It primarily focuses on OFDM and evaluates various performance metrics like Bit Error Rate (BER), Complementary Cumulative Distribution Function (CCDF), PAPR, and the 64-QAM constellation diagram in different HST speeds. The study includes a comprehensive analysis of the HST channel and its integration with the DVB-Terrestrial system. Key findings demonstrate how higher speeds result in increased PAPR values and changes in the 64-QAM constellation diagram, indicating the necessity for robust power amplifiers and efficient symbol detection methods. The paper also shows that while higher HST speeds generally lead to worse BER values, the performance of channel coding can mitigate this effect to some extent. The research provides significant insights for optimizing DVB-Terrestrial communication systems in HST environments, highlighting the importance of channel coding and modulation in maintaining signal quality and system efficiency.

Keywords: Channel model, Doppler shift, DVB-terrestrial, High-speed Train, OFDM.

1. Introduction

Orthogonal frequency division multiplexing (OFDM) is a popular modulation for wireless communication because it can transmit data quickly over a wide bandwidth while being resistant to interference [1]. OFDM is suitable for digital video broadcasting (DVB) [1], because of its high data rates and OFDM has the capability for eliminating inter-symbol interference (ISI) between OFDM symbols by cyclic prefix (CP) [2]. OFDM has high data rates, so the higher-order modulation schemes allow us to transmit more data, but they are also more susceptible to errors [3]. To achieve a high data rate and minimize the error rate, forward error correction (FEC) is used for channel coding. One of the methods for channel coding is using Reed-Solomon (RS) coding. It increases the performance of the bit error rate (BER) of limited and power-limited channels by the addition of redundancy to the transmitted data.

OFDM systems need allocation of guard bands between subcarrier frequencies to avoid inter-symbol interference (ISI) [4]. A discrete wavelet transform – orthogonal frequency division multiplexing (DWT-OFDM) could combat narrowband interference better than the traditional Discrete Fourier Transform (DFT) and tougher in inter-carrier interference (ICI). This research proposes a combination of DWT with differential amplitude phase shift keying (DAPSK) modulation scheme for reducing peak-to-average power ratio (PAPR) in OFDM systems for digital video broadcasting terrestrial (DVB-Terrestrial).

DVB-Terrestrial technology defines the framing, modulation, channel, and noise elimination techniques for digital television broadcasting over terrestrial channels [5]. This research provides a

transmission process that focuses on the receiver section based on the OFDM system. DVB-Terrestrial networks offer greater flexibility, efficiency, and robustness in terms of power consumption, bandwidth, and network coverage, which enables the launch of new and innovative services.

DVB networks are typically designed to deliver high-quality TV signals to fixed locations with rooftop antennas, rather than mobile devices. It might not provide a good coverage level for vehicular mobile reception [6]. To improve the mobile performance of DVB-Terrestrial, it deployed receive antenna diversity, hierarchical modulation, and application layer–forward error correction (AL-FEC). This research [6] shows that a combination of these solutions can maintain a good signal quality even when the receiver is moving at high speeds or in areas with poor signal reception. Meanwhile, the consideration of channel coding and modulation used was presented in DVB-Terrestrial mobile communications [7].

In high-speed train (HST) communication technology development, there are several methods for improving the quality of communication. Reliable high-speed wireless communication, especially in 5G communications has been discussed [8]. OFDM has become popular choice for wideband communication because it is efficient in the spectrum usage and robust to multipath interference, and it is suitable for high-speed trains communication. Meanwhile, long-term evolution (LTE) for railway communications has adopted the OFDM [9], [10]. It allows for seamless communication from cellular networks to 5G, enabling high-mobility communication. The information of relative locations and velocities between corresponding antenna pairs shows that ICI in additive white Gaussian noise (AWGN) and Rician channel could be mathematically calculated [10].

The HST channel is nonstationary, which means that its statistical properties change over time. This is due to the high mobility of the train and the fact that the train passes through different types of environments, such as tunnels, viaducts, hilly terrains, and open spaces. As a result, the channel can exhibit different types of fading, such as shadowing and multipath fading, which can affect the quality of wireless communication. The HST channel is a channel model that can capture the nonstationary of the HST channel by incorporating both large-scale and small-scale fading parameters. This model can be used to design and evaluate wireless communication systems on high-speed trains and other types of vehicular communication networks. Also, this channel used a geometric-based stochastic model (GBSM) that represents the channel as a tapped delay line (TDL) structure, where the taps are represented by multiple confocal ellipses with the base station (BS) and mobile relay station (MRS) located at the foci. The ellipses used in this model are confocal, which means that they share the same foci, and their shapes and sizes are determined by channel parameters such as delay spread, Doppler spread, and angle of arrival (AoA). This channel model has never been simulated and integrated with a DVB-Terrestrial communications system before.

The contribution of this paper is in terms of the use of DVB-Terrestrial technology which is implemented directly on HST channels as a result of GBSM-based channel modeling. As far as the author observes, this is the first paper to use the results of HST channel modeling integrated with a DVB-Terrestrial communication system. This will produce significant differences, considering that the characteristics of the HST channel used have never been studied before to be combined with other communication systems. In this paper, performance parameters in the form of bit error rate (BER) will be measured for predetermined signal to noise ratio (SNR) values, using various vehicle speed scenarios, in this case, high-speed trains. Apart from that, analysis will also be carried out regarding the Complementary Cumulative Distribution Function (CCDF), Peak to Average Power Ratio (PAPR), and the 64-QAM constellation diagram in OFDM communications for DVB-Terrestrial applications.

The organization of the paper consists of background which has been described in Section I of the Introduction, Related Works in Section II, Research Method and HST Channel Model are explained in Section III, Section IV focuses on the Results and Discussion, and Conclusions are discussed in Section V.

2. Related works

Several studies that have been carried out related to HST channel models and DVB technology are in this section. The research undertaken by [11] introduces a novel method for estimating the frequency offset resulting from the Doppler shift. This method effectively distinguishes the path with the Line of Sight (LOS) component from the multipath channel. The simulation results demonstrate that the suggested scheme surpasses the existing schemes in terms of mean square error. This research differs from our previous study in terms of

the implementation of the HST channel model, which was executed in a more straightforward manner. The HST channel in this research exclusively supports multipath propagation characterized by Rayleigh and Rician distribution models. The HST channel model exhibits a more intricate structure by incorporating multiple levels of multipath propagation inside the current elliptical layers.

Other research on HST channels with Digital Video Broadcasting – Second Generation Terrestrial (DVB-T2) communication systems was carried out in [12]. This paper discussed a beamforming-based receiver for the DVB-T2 system in a HST environment. The authors have proposed a new signal processing scheme to effectively suppress interference caused by multiple Doppler frequency offsets and channel variations. The simulation results show that the proposed beamforming-based DVB-T2 receiver scheme is effective in suppressing interference in the received signal in the HST environment. The BER performance of the proposed scheme is better than that of the conventional DVB-T2 receiver, and the gain in SNR by the proposed scheme is more than 20 dB. The disparity between this research and the written publication lies in the block diagram of the communication system employed and the HST channel model. The previous research utilized a communication system block diagram that lacked a channel coding function, such as the regularly employed Low-Density Parity Check (LDPC) or Reed Solomon in DVB-Terrestrial. In addition, the HST channel is simplified by disregarding the multipath level utilized. Another paper discussing DVB-T2 whose mobile user is carried out by [3]. The author investigates the efficiency of DVB-T2 and DVB-T2-Lite in mobile receivers, specifically in relation to the TU6 mobile channel in sub-urban regions. The paper demonstrates that inter-frame interleaving offers a substantial performance benefit, particularly when mobile speeds are poor. In addition, DVB-T2-Lite with lower coding rates can surpass DVB-T2 at extremely high speeds. The channel model employed in this paper is mobile, namely in a suburban setting. The mobile channel model employed in this work has a slower velocity compared to the HST channel model. Consequently, the utilization of the HST channel at a significantly greater speed leads to distinct variations in the BER parameter values.

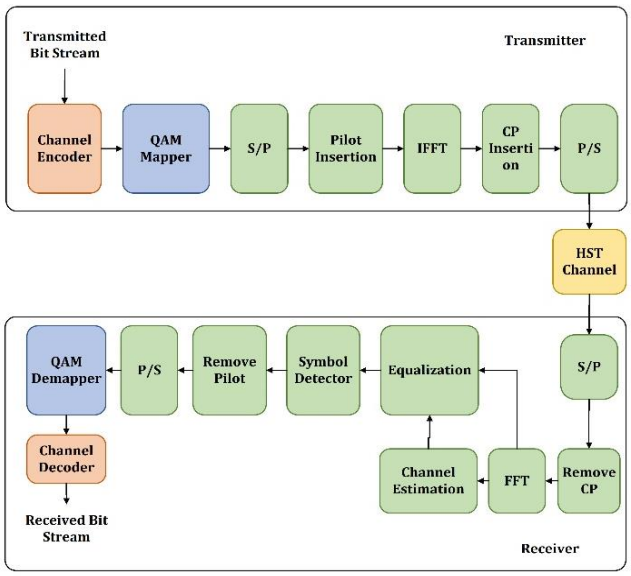

Figure. 1 Block Diagram of Proposed DVB-Terrestrial Communication Systems using HST Channel

3. Research method

3.1 System model

Figure 1 shows the block diagram of the DVB-Terrestrial system using HST channel. This block diagram shows the DVB-Terrestrial communication system which is integrated with OFDM multicarrier using the proposed HST channel model.

A. High-Speed Train (HST) Channel Model

The HST channel modeling using the DVB-Terrestrial antenna can be shown in Fig. 2 below. It can be stated using numerous equations based on Fig. 2 that represent the form of HST communication utilizing the DVB-Terrestrial antenna. With reference to Ghazal's research, the HST channel integrated in this study employs a geometry-based stochastic model (GBSM) nonstationary channel model [13]. A channel model with three ellipses, single bounce (SB) components, and a LOS component [13]. Taps are depicted as several ellipses with the BS and DVB-Terrestrial antennas in the center, based on the tapped delay line (TDL) structure. The total number of ellipses or taps is represented by the variable i, and there are multiple scatterers, Ni.

Equations (1), (2), and (3) below represents the LOS component $h_{1,rs}^{LOS}(t)$ and the SB component $h_{1,rs}^{SB}(t)$, respectively [13]:

$$h_{1,rs}(t) = h_{1,rs}^{LOS}(t) + h_{1,rs}^{SB}(t) \quad (1)$$

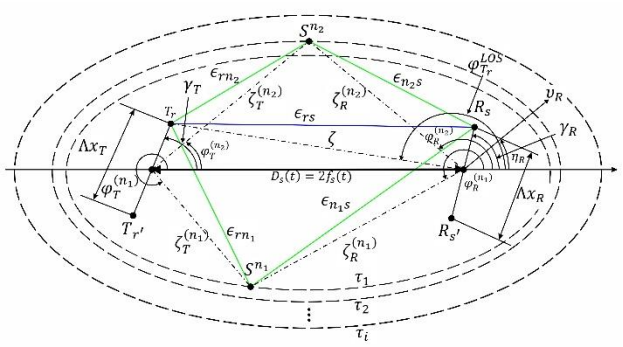

Figure. 2 HST channel model [13]

$$h_{1,rs}^{LOS}(t) = \sqrt{\frac{K_{rs}}{K_{rs}+1}} e^{-j2\pi f_c \tau_{rs}(t)} e^{j2\pi f_{max} t\, cos\left(\phi_{T_r}^{LOS}(t)-\eta_R\right)} \quad (2)$$

$$h_{1,rs}^{SB}(t) = \sqrt{\frac{\Phi_{i,rs}}{K_{rs}+1}} \lim_{N_1\to\infty} \sum_{n_1=1}^{N_1} \frac{1}{\sqrt{N_1}} e^{-j\left(\vartheta_{n_1}-2\pi f_c \tau_{rs,n_1}(t)\right)} \times e^{j2\pi f_{max} t\, cos\left(\varphi_R^{(n_1)}(t)-\eta_R\right)} \quad (3)$$

where the discrete propagation delay of the i-th tap is represented by τ_i and complex ST-variant tap coefficient is represented by $h_{1,rs}(t)$. The complex tap coefficient for taps other than the first tap $(1 < i \leq I)$ of the $T_r - R_s$ link the sum of the SB components only. Since there are three taps or ellipses employed in this study, I = 3, which means that i = 2 and 3. The complex equation for the other taps is shown in Eq. (4) below [13]:

$$h_{i,rs}(t) = h_{i,rs}^{SB}(t) = \sqrt{\Phi_{i,rs}} \lim_{N_i\to\infty} \sum_{n_i=1}^{N_i} \frac{1}{\sqrt{N_i}} e^{-j\left(\vartheta_{n_1}-2\pi f_c \tau_{rs,n_i}(t)\right)} \times e^{j2\pi f_{max} t\, cos\left(\varphi_R^{(n_1)}(t)-\eta_R\right)},\ 1 < i < I \quad (4)$$

The system becomes stationary when the parameters in Eqs. (2), (3), and (4) fluctuate with time $\tau_{rs}(t)$, $\varphi_{T_r}^{LOS}(t)$, $\tau_{rs,n_i}(t)(i = 1, 2, \dots, I)$, and $\varphi_R^{(n_1)}$. The value of $\Phi_{i,rs}$ indicates the average power for the i-th tap. The value of $\tau_{rs}(t) = \epsilon_{rs}(t)/c$ and $\tau_{rs,n_i}(t) = \left(\epsilon_{rn_i}(t) + \epsilon_{n_i s}(t)\right)/c$ is the respective wave travel time through $T_r - R_s$ link and $T_r - s^{(n_i)} - R_s$ link.

B. HST Channel Validation

1) Probability Density Function (PDF)

The probability function that depicts the density of a continuous random variable falling within a particular range of values is known as the Probability Density Function (PDF). It is sometimes referred to as the cumulative distribution function (CDF). PDF is defined for continuous random variables [14]. When a continuous random variable is involved, let F(x) be the CDF of X. Then the formula for the PDF, f(x), is given in Eq. (5) [14]:

$$f(x) = \frac{dF(x)}{dx} = F'(x) \quad (5)$$

2) Complementary Cumulative Distribution Function (CCDF)

Integral computation of the PDF to derive the CDF. Ultimately, the Complementary CDF (CCDF) is obtained by inverting the CDF [15]. Power CCDF curves are defining the power characteristics of the signals that are amplified, encoded, mixed, and transmit over communication systems. Generally, the CDF and CCDF of a continuous or discrete signal, X, is stated in Eqs. (6) and (7) below [14]:

$$F_X(x) = P(X \leq x) = \int_{-\infty}^{x} f(t)dt \quad \text{for } x \in \mathbb{R} \quad (6)$$

The CCDF is formulated as in Eq. (7) below [14]:

$$\bar{F}_X(x) = P(X > x) = 1 - F_X(x) \quad (7)$$

A plot of relative power levels vs probability is called a CCDF curve [15].

3) Peak to Average Power Ratio (PAPR)

The OFDM signal is produced by subjecting data symbols to an Inverse Fast Fourier Transform (IFFT). There is a high possibility that a subset of these symbols adds up coherently, leading to the production of some large peaks at the output. This phenomenon is usually quantified in terms of PAPR, which is proportional to the number of subcarriers [16]. High PAPR can decrease the SNR while diminishing power amplifier performance. As a result, RF power amplifiers must be operated in a very large linear region then signal peaks will enter the non-linear region, causing distortion [17].

The PAPR of the OFDM symbol is defined as the ratio between the maximum power of the OFDM symbol and the average power of the OFDM symbol [18]. The PAPR of the OFDM sequence x[n], which we denote as PAPR{x[n]}, can be defined in Eq. (8) as follows [19]:

$$PAPR\{x[n]\} = \frac{P_{peak}}{P_{average}} = \frac{max|x[n]|^2}{E\{|x[n]|^2\}} \quad (8)$$

with $x[n]$ is an OFDM signal after IFFT (for N sub-carriers), $E\{.\}$ is the expectation operator, and the denominator is the average power of $x[n]$ over $0 \leq n \leq N-1$.

The CCDF is typically used instead of the CDF to assess the possibility that the PAPR of a certain data block will exceed the specified threshold. The CDF is described in Eq. (9) below [20]:

$$CDF = F(z) = 1 - e^{-Z} \quad (9)$$

with Z as the threshold value. The CCDF refers to the probability that the PAPR value of the OFDM symbol is greater than or equal to a specific threshold Z [21]:

$$CCDF = P\{PAPR > Z\} \quad (10)$$

Based on Eqs. (9) and (10), the relationship between CDF, CCDF, and PAPR is obtained as follows [20]:

$$P\{PAPR > Z\} = 1 - P\{PAPR \leq Z\} = 1 - F(z)^N = 1 - (1 - e^{-Z})^N \quad (11)$$

C. DVB-Terrestrial Using OFDM Multicarrier

DVB-Terrestrial with the use of OFDM, was standardized by the European Telecommunications Standards Institute (ETSI) [22]. The use of OFDM requires Fast Fourier Transform (FFT) and Inverse Fast Fourier Transform (IFFT) for generating sub-carrier frequency by applying the orthogonality principle. Multicarrier modulation (MCM) with N sub-carriers, frequency f_k and each k-th sub-carrier transmits a complex symbol $\{d_i\}_{k=1}^{N}$ which produces a transmit signal [23]:

$$s(t) = \sum_{i=1}^{k} [I\ cos(2\pi f_k t) + Q\ sin(2\pi f_k t)] \quad (12)$$

$$s(t) = \sum_{i=1}^{k} Re\{d_i e^{j2\pi f_k t}\};\ 0 \leq t \leq T_{sym} \quad (13)$$

with $f_k = f_c + k\Delta f$ and k = 0, 1, 2, …, N-1. Notation N is the number of subcarriers with a distance between sub-carriers of Δf.

For wide channels, the symbol duration is smaller than the delay distribution τ, so inter-symbol interference (ISI) occurs. So that a channel does not experience ISI, the symbol frequency ($1/T_{sym}$) must be greater than the delay distribution (τ) of the channel. To overcome this problem, the MCM splits the bit stream with a high speed in parallel into L sub-streams with a lower speed, namely R/L, through a serial to parallel (S/P) conversion process, so that each sub-stream has symbol duration $T_{sym}/L >> \tau$.

D. Channel Coding

1) Reed Solomon (RS)

Nonbinary codes consisting of m-bit sequences as symbols are known as Reed Solomon (RS). An integer m can be any positive number greater than 2. There are RS (n, k) codes on m-bit symbols for every n and k considering this condition [24]:

$$0 < k < n < 2^m + 2 \quad (14)$$

where k is the number of data symbols being encoded, and n is the total number of code symbols. For the most conventional RS (n, k) code [24]:

$$(n, k) = (2^m - 1, 2^m - 1 - 2t) \quad (15)$$

where t is the symbol-error correcting capability of the code, and $n - k = 2t$ is the number of parity symbols. The code can correct any combination of t or fewer errors, where t can be expressed as [24]:

$$t = \left[\frac{n-k}{2}\right] \quad (16)$$

Equation (16) illustrates that correcting t symbol errors requires no more than $2t$ parity symbols.

2) Convolutional Coding

Convolutional Coding (CC) describes how the information bits are modulated with a convolution code and sent through a linear finite-state shift register by the encoder to convert k-bit information into an n-bit codeword [25]. N binary addition operations and K-stage shift registers with k bits per stage make up the encoder structure. By adding bits from each step in binary order, each bit produces an output codeword. The encoder's constraint length is KK, its coding rate is k/n, and its total possible states are $2(K-1)k$ [26].

3) Viterbi Decoding

By employing an asymptotically optimal decoding strategy, the Viterbi decoding is the most comprehensive decoding method for convolutional codes. The Viterbi decodes the bit stream and fixes the faults by utilizing the redundancy imposed by the convolutional encoder [27]. By using the Viterbi algorithm, CC-based on the Trellis diagram can be decoded using either hard-decision or soft-decision decoding. When decoding with challenging decisions, the Viterbi approach finds the path across the trellis diagram with the smallest Hamming distance from the received sequence. Soft-decision decoding selects the path from the input sequence that produces the smallest Euclidean. Hard-decision decoding involves determining the Hamming distance for a given path in a Trellis diagram. The decoder chooses the data sequence from the route with the shortest Hamming distance [28].

3.2 DVB-Terrestrial system in HST environment

There are several Digital Terrestrial Television standards, including Digital Video Broadcasting – Terrestrial. At the DVB-Terrestrial transmitter, several programs can be packaged into a physical layer pipe (PLP). Even, in a multi-PLP systems, several PLP are packaged further into a baseband (BB) frame format. This format is transmitted using OFDM modulation, where a stream of bits is split into several sub-streams, each of which modulates a dedicated sub-carrier frequency [29].

In the HST environment, the signals from different BS will travel through different channels and experience different Doppler shifts in the transmission. The received signal at the receiver will be a signal with multiple Doppler frequency offsets and different time-varying channels [12]. One of the main parameters related to mobile performance is the FFT size due to its relation with the influence of Doppler spread. Smaller FFT size improves the performance. Some Doppler frequency examples at a 600 MHz RF channel frequency of are [30]:

- For highway speed, 130 km/h or 80 mph, 72 Hz. 4K FFT should be used.
- For high-speed trains, 250 km/h or 155 mph, 139 Hz. 4K FFT can still be used but with QPSK 2/3.

In OFDM-based DVB-Terrestrial systems, the orthogonality is not guaranteed in the presence of the Doppler effect. The Doppler spreading of the transmitted signal produces the ICI, which degrades the performance of OFDM systems [31]. In DVB-Terrestrial communication, the transmission quality improves with additional channel coding (CC and RS) and using modulation 64-QAM. DVB-Terrestrial OFDM subcarriers form channels or sub-groups, Physical Layer Pipes (PLP) with different parameters, such as modulation type, the code rate, interleaving, etc. [32].

Table 1. Simulation parameters

No	Parameter	Notations	Values
1	Carrier frequency	fc	2.6 GHz, 470 MHz
2	Symbol duration	Ts	10 μs – 200 μs
3	Train Speeds	v_R	5 m/s, 50 m/s, 100 m/s
4	FFT size	N	2048
5	Max delay spread	τmax	5.6 μs
6	Distance range	D(t)	250m;1550m
7	Initial distance	D(to)	800 m
8	Rician factor	K	5.9
9	Modulation	M	64 QAM
10	Bandwidth	L	8 MHz
11	Channel Model	H	HST Channel
12	Max Doppler Freq.	Fd	156 Hz for 360 km/h

3.3 Simulation parameters

The simulation parameters utilized in this study are listed in Table 1.

4. Result and discussion

4.1 CCDF and PAPR analysis

The CCDF in the field of wireless communications is a statistical function that measures the probability that a certain signal power, will exceed a specific threshold value. It is particularly useful in the analysis and design of wireless communication because it helps in understanding the characteristics of signal variation, known as fading. The CCDF is plotted as a graph where the vertical axis shows the probability that the power output will exceed a certain value on the horizontal axis. This graph aids in designing communication systems by considering the effects of high-power peaks and in choosing or designing equipment that can handle these peaks without causing significant losses in signal quality or system efficiency. The CCDF is also commonly used to characterize power amplifiers or to assess system performance in terms of PAPR. The CCDF provides insight into how often and by how much the signal peaks exceed the average power of the signal. This is crucial because in many communication systems, like OFDM, high PAPR can cause nonlinear

distortion in power amplifiers and decrease the overall system efficiency.

In a wireless channel, the relationship between the user's speed and the CCDF is related to the variability of the signal, which affects the distribution of the signal's amplitude or power. As the speed of a user increases, particularly in mobile scenarios such as in a car or train, the characteristics of the wireless channel change more rapidly due to the Doppler effect and fast fading. The Doppler effect causes the frequency of the signal received to vary depending on the speed of the user relative to the transmitter, which can lead to a spread in the signal's spectrum known as Doppler spread. Fast fading occurs when the amplitude and phase of the signal change rapidly over short periods of time or travel distances, which is more pronounced at higher speeds. These changes can lead to a higher variability in the received signal power. Consequently, the CCDF of a high-mobility user's signal might show a higher probability of signal peaks exceeding a certain threshold compared to a stationary or slow-moving user. This is because the fast variations in the signal can lead to more frequent and higher peaks in signal power.

a. HST speed (v_r) of 5 m/s

In this section, we analyze the relationship between HST speed and CCDF. There are 3 speeds compared, namely at 5 m/s which represents low speed, 50 m/s represents medium speed, and 100 m/s represents high speed. CCDF results at a speed of 5 m/s can be shown in the Fig. 3 below. At this speed, signal values that are more than 10.552 dB have a probability of 0.0001 as shown in the black graph. This value is worse than the average signal obtained when using the AWGN channel which is shown in the blue graph. This condition will vary if the speed is changed so that the HST channel also changes.

The PAPR value produced at this speed is 10.553 dB, as shown in Fig. 4. High PAPR values indicate that at times, the signal can have very high peaks compared to its average level. This is common in modulation schemes like OFDM used in modern wireless communication systems like LTE and DVB. In practical terms, a high PAPR can be challenging for wireless communication systems because it requires the power amplifier to operate efficiently over a wide dynamic range to accommodate the high peaks without distortion. Power amplifiers with high linearity are needed to handle high PAPR signals without incurring

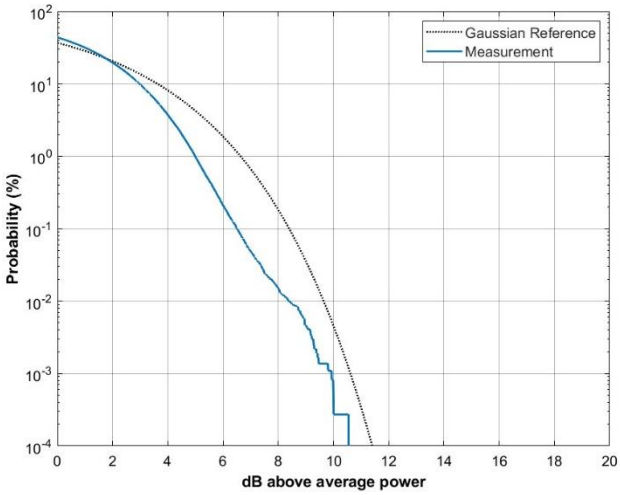

Figure. 3 CCDF at a speed of 5 m/s

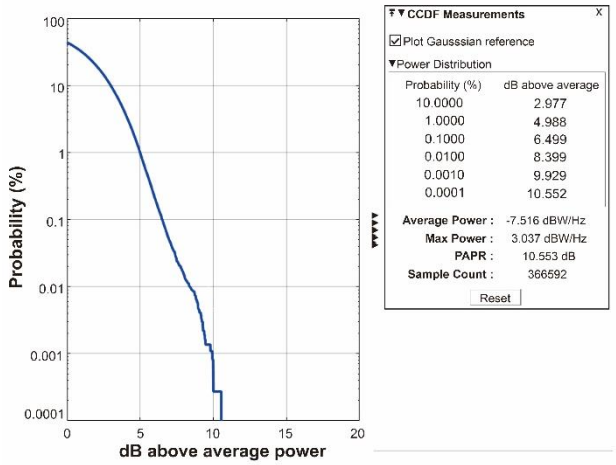

Figure. 4 PAPR at a speed of 5 m/s

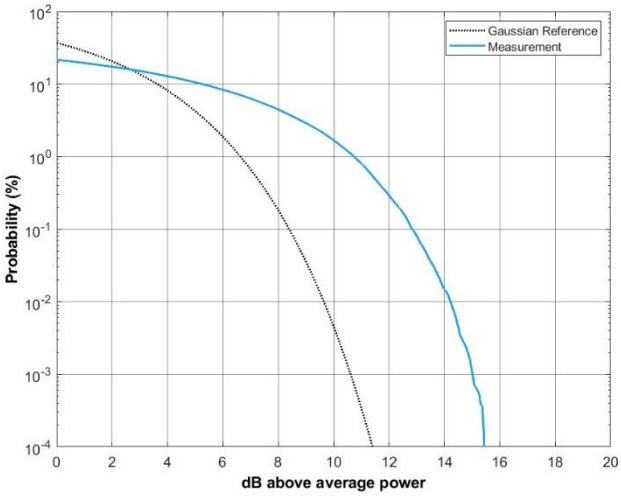

Figure. 5 CCDF at a speed of 50 m/s

significant distortions, which can be more expensive and less power efficient.

b. HST speed (v_r) of 50 m/s

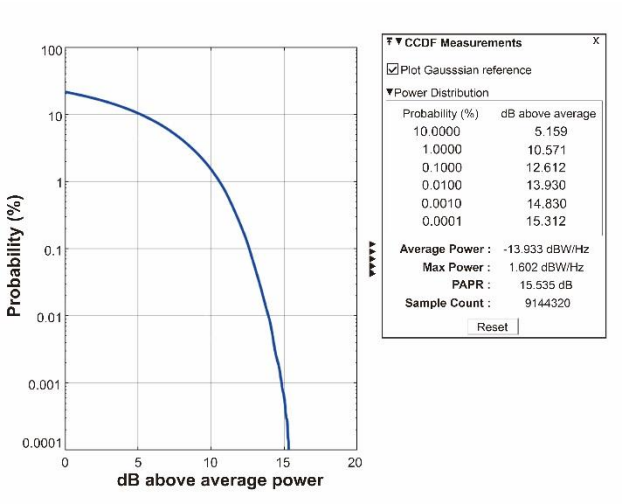

Figure. 6 PAPR at a speed of 50 m/s

If the speed of the train is increased 10 times from the first scenario, the CCDF graph against speed changes as the signal limit value increases beyond the AWGN channel as in the Fig. 5. This shows that at higher speeds, the CCDF value becomes better due to the channel coding embedded in the communication system The role of this coding channel will improve the CCDF value which should be worse at higher speeds to better CCDF value. The CCDF value of the HST channel in this condition has a value of 15.312 with the smallest probability of 0.0001.

The PAPR value is calculated to be 15.535 dB at a speed that is 10 times faster than the prior value of approximately 5 dB. It is shown in Fig. 6. This demonstrates that the PAPR value will increase as the speed of the fast train increases. This result increases in the disparity between the strongest and weakest signals. This can be foreseen by designing the power amplifier appropriately to prevent linear distortion. The existence of channel coding used in the communication system cannot overcome the increase in PAPR due to the increase in HST speed.

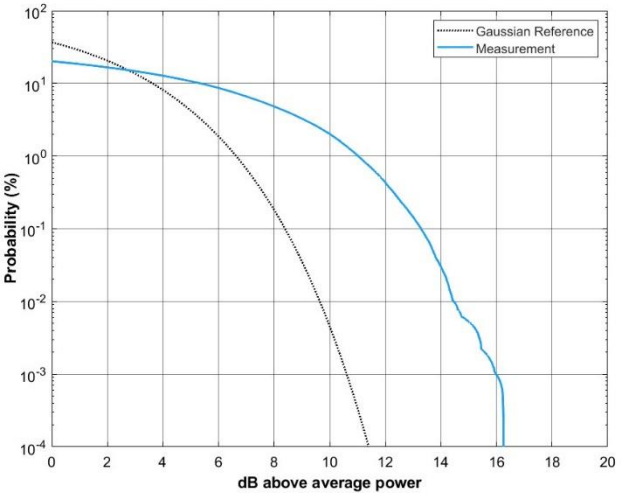

Figure. 7 CCDF at a speed of 100 m/s

c. HST speed (v_r) of 100 m/s

If we increase the HST speed twice from the second speed scenario, it will produce a CCDF graph as in the following Fig. 7. The CCDF value has a limit of 16.249 dB with a probability of 0.0001 or higher than the CCDF in the previous speed scenario. This can occur due to the influence of channel coding which overcomes the non-linearity of the HST communication channel, resulting in CCDF values at higher speeds. RS codes are a type of error-correcting code (ECC) that are particularly effective in correcting burst errors including those used in Digital Video Broadcasting (DVB). In DVB, data can be corrupted due to various reasons like noise, interference, or signal fading. RS codes can correct these errors effectively, ensuring the integrity of the received data.

The PAPR value produced in this highest speed scenario (100 m/s) can reach a value of 16.255 dB, as described in Fig. 8 below. This results in a higher value than the PAPR of the previous speed scenario. This can happen because, in the block diagram of the communication system used, there is no PAPR mitigation method. There are various techniques specifically designed to reduce PAPR in OFDM systems. These include clipping and filtering, selective mapping (SLM), partial transmit sequences (PTS), and coding techniques. However, these techniques are not the same as channel coding used for error correction.

4.2 The 64-QAM constellation diagram

a. HST speed (v_r) of 5 m/s

In this study, we used 64-QAM modulation. This

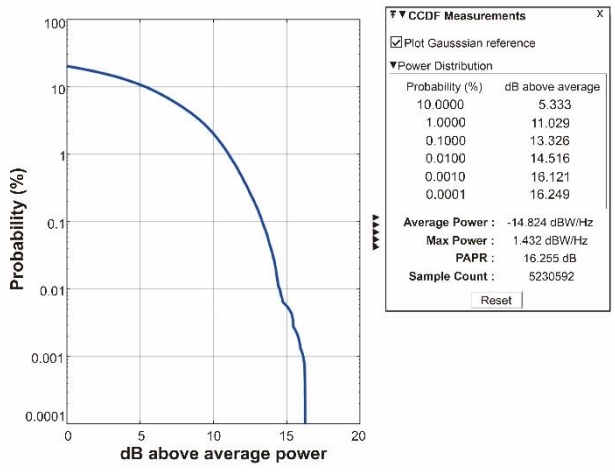

Figure. 8 PAPR at a speed of 100 m/s

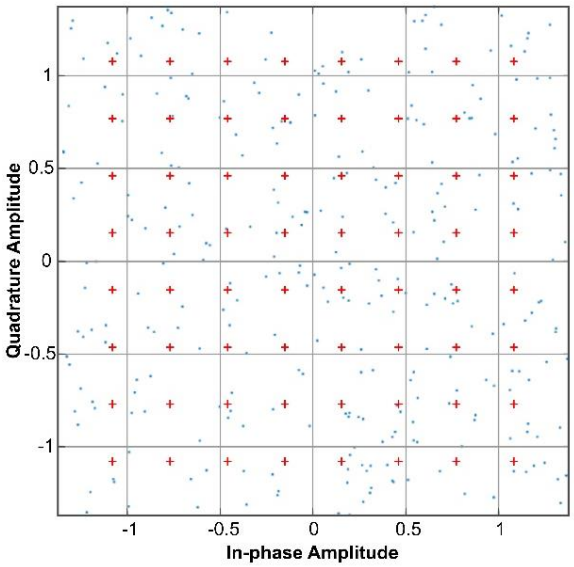

Figure. 9 The 64-QAM constellation diagram at a speed of 5 m/s

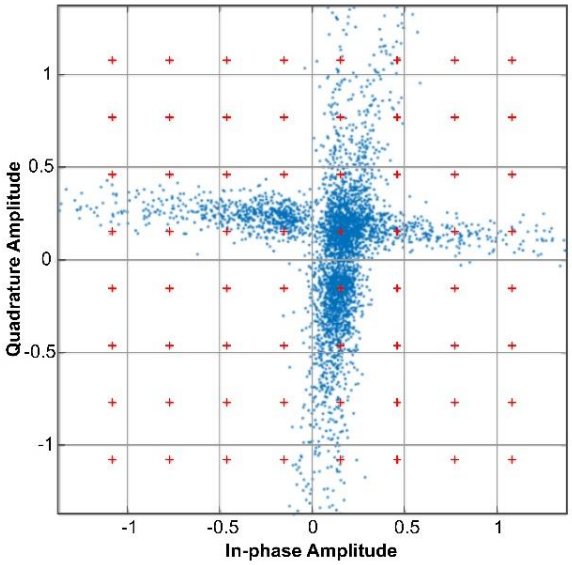

Figure. 10 The 64-QAM constellation diagram at a speed of 50 m/s

modulation scheme can transmit 6 bits per symbol, as it has 64 distinct states or symbols in the constellation diagram. This allows for a higher data rate, making it suitable for applications requiring high bandwidth, such as high-definition television (HDTV) broadcasting.

With its higher number of symbols, 64-QAM is more sensitive to noise and interference. The symbols in the constellation diagram are closer each other, so it's easier for noise to cause errors in symbol interpretation. The use of 64-QAM in DVB-Terrestrial represents a trade-off. While it allows for higher data rates, it is less robust against channel impairments compared to simpler modulation schemes. The choice of using 64-QAM would depend on the desired balance between throughput and transmission robustness. In the constellation diagram at Fig. 9 above, the speed scenario is 5 m/s and the condition of the channel which has multipath has caused the symbols to spread from their proper position. The distribution of this symbol will have a pattern as the speed increases in the next scenario.

b. HST speed (v_r) of 50 m/s

In the speed scenario which is up to 10 times higher than the first scenario, the constellation diagram graph appears to have improved due to the RS channel coding used in the communication system. The constellation diagram appears to produce symbols that form a clustered pattern to produce a thicker line at a certain coordinate area, see Fig. 10. This is easier to anticipate than the previous constellation diagram which forms a more random and un-patterned symbol distribution pattern. These known spreading patterns help in channel estimation and synchronization, which are crucial for accurate symbol detection in 64-QAM.

c. HST speed (v_r) of 100 m/s

In the highest-speed scenario, the graphic pattern of the constellation diagram increasingly produces a symbol distribution pattern that becomes smaller and forms thinner lines. It can be described in Fig. 11. This happen because the performance of the RS channel coding works better in high-speed scenarios. With a more patterned symbol distribution pattern, it will facilitate the symbol detection process on the receiver side.

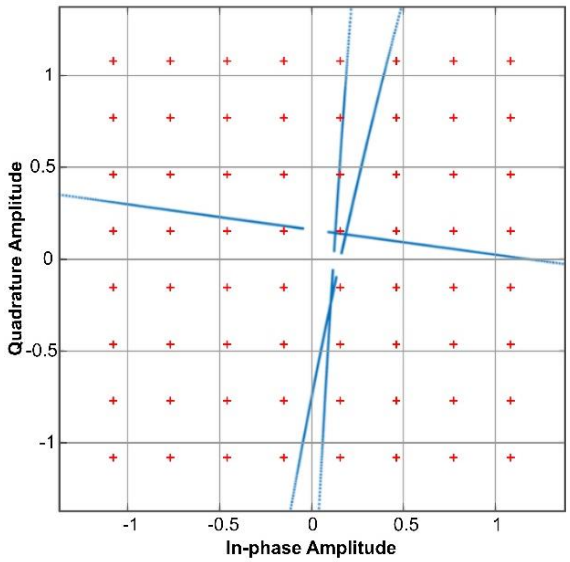

Figure. 11 The 64-QAM constellation diagram at a speed of 100 m/s

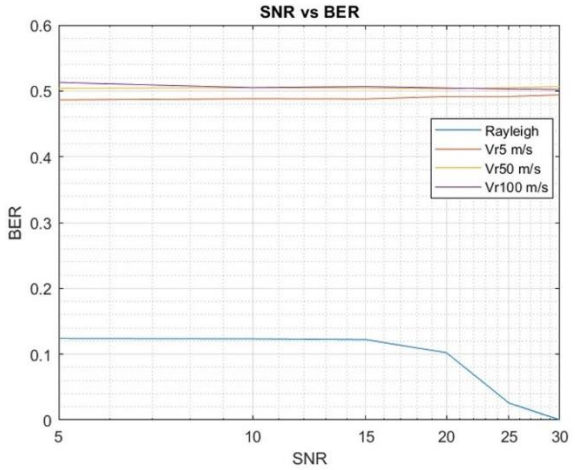

Figure. 12 BER performance of all HST speed scenarios

4.3 Bit error rate analysis

In this section, we investigated the relationship between HST speed and the resulting BER. This graph contains the 3-speed scenarios and a comparison with the BER graph on the Rayleigh channel. This graph is used to validate 3 graphs from 3 different speed scenarios. On the Rayleigh channel graph, we set the HST speed to zero or not moving. This will result in the BER value on the Rayleigh channel having the best value among all existing graphs. The comparison results of the BER graph with HST speed can be seen in Fig. 12. From this graph the smallest speed scenario, namely 5 m/s, has a better BER value for each SNR compared to the other 2 speed scenarios. This naturally occurs because greater speed will produce worse BER values. However, if we look at the values of the other 2 speed scenarios, the difference in BER is very small. This can occur due to the performance of channel coding when correcting HST channels with non-linear burst error characteristics.

5. Conclusion

We have analyzed and emphasized the critical impact of high-speed train (HST) environments on the performance of DVB-Terrestrial systems. In detail, the influence of HST channel on CCDF, PAPR, and BER parameters has been analyzed in this research. We use a geometric channel model that has never been used before to be integrated with a DVB-Terrestrial communication system. The performance of the channel coding used in this research affects improving the performance of CCDF parameters at higher train speeds, resulting in better CCDF values. This is demonstrated by the CCDF data, which show that at a speed of 5 m/s, the smallest probability of 0.0001 yielded a value of 10.552 dB, while at speeds of 50 m/s and 100 m/s, it grew to 15.312 dB and 16.249 dB. In addition, the PAPR parameters will get worse as the train speed increases. According to the research findings, at speeds of 5 m/s, 50 m/s, and 100 m/s, the PAPR values were higher (worse) at 10.553 dB, 15.535 dB, and 16.255 dB, respectively. This study was not equipped with PAPR mitigation. The influence of RS channel coding makes the 64-QAM modulation diagram constellation better when the train speed increases sharply.

Conflicts of Interest

The authors declare no conflict of interest.

Author Contributions

The contributions of the author are elaborated as follows. Anggun Fitrian Isnawati: conceptualization, methodology, writing review, and supervision; Wahyu Pamungkas: validation and analysis; M. Panji Kusuma Praja: introduction, visualization, and editing.

Acknowledgments

The authors would like to express a gratitude to the Directorate General of Higher Education, Research and Technology for sponsoring this research through the 2023 National Competitive Basic Research Grants.

References

[1] A. M. Khan, V. Jeoti, and M. A. Zakariya, “Improved pilot-based LS and MMSE channel estimation using DFT for DVB-T OFDM systems”, In: *Proc. of 2013 IEEE Symposium on Wireless Technology & Applications (ISWTA)*, Kuching, Malaysia, pp. 120–124, 2013, doi: 10.1109/ISWTA.2013.6688752.

[2] H.i Yang, “A road to future broadband wireless access: MIMO-OFDM-Based air interface”, *IEEE Commun. Mag.*, Vol. 43, No. 1, pp. 53–60, 2005, doi: 10.1109/MCOM.2005.1381875.

[3] D. Parida, M. Nayak, and D. Dash, “An efficient forward error correction based OFDM technique for digital video broadcasting”, In: *Proc. of 2017 International Conference on Communication and Signal Processing (ICCSP), Chennai*, pp. 1195–1199, 2017.

[4] Y. A. Lafta and P. Johnson, “High performance OFDM systems for digital video broadcasting-terrestrial”, *International Journal of Digital*

Information and Wireless Communications, Vol. 2, No. 1, pp. 66–74, 2012.

[5] N. Alhyani, "Efficient Terrestrial Digital Video Broadcasting Receivers Based OFDM Techniques", *ELECTROTECHNICAL REVIEW*, Vol. 1, No. 11, pp. 76–79, 2021, doi: 10.15199/48.2021.11.13.

[6] J. Lopez-Sanchez, *D. Gomez-Barquero, D. Gozalvez, and N. Í. S. Cardona*, "On the Provisioning of Mobile Digital Terrestrial TV Services to Vehicles With DVB-T", *IEEE Trans. on Broadcast.*, Vol. 58, No. 4, pp. 642–647, 2012, doi: 10.1109/TBC.2012.2202034.

[7] U. Ladebusch and C. A. Liss, "Terrestrial DVB (DVB-T): A Broadcast Technology for Stationary Portable and Mobile Use", *Proc. IEEE*, Vol. 94, No. 1, pp. 183–193, 2006, doi: 10.1109/JPROC.2005.861009.

[8] Y. Liu, C.-X. Wang, and J. Huang, "Recent Developments and Future Challenges in Channel Measurements and Models for 5G and Beyond High-Speed Train Communication Systems", *IEEE Commun. Mag.*, Vol. 57, No. 9, pp. 5056, 2019, doi: 10.1109/MCOM.001.1800987.

[9] G. Tingting and S. Bin, "A high-speed railway mobile communication system based on LTE", In: *Proc. of 2010 International Conference on Electronics and Information Engineering*, Kyoto, Japan, pp. V1-414-V1-417, 2010, doi: 10.1109/ICEIE.2010.5559665.

[10] J. Lu, *X. Chen, S. Liu, and P. Fan*, "Location-Aware ICI Reduction in MIMO-OFDM Downlinks for High-Speed Railway Communication Systems", *IEEE Trans. Veh. Technol.*, Vol. 67, No. 4, pp. 2958–2972, 2018, doi: 10.1109/TVT.2017.2702186.

[11] L. Yang, G. Ren, and Z. Qiu, "A Novel Doppler Frequency Offset Estimation Method for DVB-T System in HST Environment", *IEEE Trans. on Broadcast.*, Vol. 58, No. 1, pp. 139–143, 2012, doi: 10.1109/TBC.2011.2170609.

[12] L. Yang, G. Ren, W. Zhai, and Z. Qiu, "Beamforming Based Receiver Scheme for DVB-T2 System in High Speed Train Environment", *IEEE Trans. on Broadcast.*, Vol. 59, No. 1, pp. 146–154, 2013, doi: 10.1109/TBC.2012.2221612.

[13] A. Ghazal, C.-X. Wang, B. Ai, D. Yuan, and H. Haas, "A Nonstationary Wideband MIMO Channel Model for High-Mobility Intelligent Transportation Systems", *IEEE Trans. Intell. Transport. Syst.*, pp. 1–13, 2014, doi: 10.1109/TITS.2014.2345956.

[14] M. Kaptein and E. Van Den Heuvel, Statistics for Data Scientists: An Introduction to Probability, *Statistics*, and Data Analysis. in Undergraduate Topics in Computer Science. Cham: Springer International Publishing, 2022. doi: 10.1007/978-3-030-10531-0.

[15] W. Pamungkas, A. F. Isnawati, S. Larasati, A. E. Jayati, E. N. Ardina, and J. Hendry, "Channel Sounder in Indoor Environment with Multipath Fading using Software Defined Radio", In: *Proc. of 2023 IEEE International Conference on Communication, Networks and Satellite (COMNETSAT)*, Malang, Indonesia, pp. 814, 2023, doi: 10.1109/COMNETSAT59769.2023.10420747.

[16] A. M. Rateb and M. Labana, "An Optimal Low Complexity PAPR Reduction Technique for Next Generation OFDM Systems", *IEEE Access*, Vol. 7, pp. 16406–16420, 2019, doi: 10.1109/ACCESS.2019.2895415.

[17] N. Kumari and S. Kaur, "A Survey on Various PAPR Reduction Techniques in OFDM Communication Systems", *Int. Res. J. Eng. Technol. IRJET*, Vol. 2, No. 6, pp. 2428, 2015.

[18] V. S. Nagaraju, R. Anusha, and R. R. Vallabhuni, "A Hybrid PAPR Reduction Technique in OFDM Systems", In: *Proc. of 2020 IEEE International Women in Engineering (WIE) Conference on Electrical and Computer Engineering (WIECON-ECE)*, Bhubaneswar, India, pp. 364–367, 2020, doi: 10.1109/WIECON-ECE52138.2020.9398011.

[19] M. Kim, W. Lee, and D.-H. Cho, "A Novel PAPR Reduction Scheme for OFDM System Based on Deep Learning", *IEEE Commun. Lett.*, Vol. 22, No. 3, pp. 510–513, 2018, doi: 10.1109/LCOMM.2017.2787646.

[20] C. Duanmu and H. Chen, "Reduction of the PAPR in OFDM Systems by Intelligently Applying Both PTS and SLM Algorithms", *Wireless Pers Commun*, Vol. 74, No. 2, 2014, doi: 10.1007/s11277-013-1325-3.

[21] R. Jaikumar, M. A. Mukunthan, C. Arvind, R. Lavanya, and K. Srihari, "A Low complexity Spatial Mapping Assisted Companding Scheme (SMaCS) for PAPR Minimization in OFDM Systems", *Natl. Acad. Sci. Lett.*, Vol. 45, No. 6, pp. 511–515, 2022.

[22] S. Hara and R. Prasad, *Multicarrier techniques for 4G mobile communications. in Universal personal communications*, Boston: Artech House, 2003.

[23] Y. S. Cho, W. Y. Yang, C.-G. Kang, and J. Kim, *MIMO OFDM wireless communication*

with MATLAB, Singapore: John Wiley & Sons (Asia) Pte, Ltd, 2010.

[24] T. K. Moon, *Error correction coding: mathematical methods and algorithms*, Hoboken, N.J: Wiley-Interscience, 2005.

[25] S. Kalita, P. Gogoi, and K. K. Sarma, "Convolutional Coding Using Booth Algorithm For Application in Wireless Communication", *IJESS*, pp. 37–41, 2011, doi: 10.47893/IJESS.2011.1008.

[26] J. Tuominen and J. Plosila, "Asynchronous Viterbi Decoder in Action Systems", *TUCS Technical Report*, 2005.

[27] Y. Nakano, D. Umehara, M. Kawai, and Y. Morihiro, "Viterbi Decoding for Convolutional Code over Class A Noise Channel," *International Symposium on Power Line Communications and Its Applications*, pp. 97–102, 2003.

[28] M. A. Aljubouri and M. Z. Iskandarani, "Performance Evaluation of Coded OFDM Using 4QPSK and 16QAM", *JCM*, pp. 676–688, 2023, doi: 10.12720/jcm.18.11.676-688.

[29] B. Setiyanto, R. Hidayat, I. W. Mustika, and S. Sunarno, "CNR and BER Ranges for the DVB-T2 Reception-Success", *IJECE*, Vol. 7, No. 6, p. 3727, 2017, doi: 10.11591/ijece.v7i6.pp3727-3734.

[30] I. Eizmendi et al., "DVB-T2: The Second Generation of Terrestrial Digital Video Broadcasting System", *IEEE Trans. on Broadcast.*, Vol. 60, No. 2, pp. 258–271, 2014, doi: 10.1109/TBC.2014.2312811.

[31] D. A. Samo, M. Slimani, G. Baruffa, and L. Rugini, "A performance study of DVB-T2 and DVB-T2-Lite for mobile reception", *Digital Signal Processing*, Vol. 37, pp. 35–42, 2015, doi: 10.1016/j.dsp.2014.11.002.

[32] J. Vlaovic, S. Rimac-Drlje, and G. Horvat, "Overview of OFDM channel estimation techniques for DVB-T2 systems", *in 2016 International Conference on Smart Systems and Technologies (SST)*, Osijek, Croatia: IEEE, pp. 75–80, 2016, doi: 10.1109/SST.2016.7765636